Sizes and interactions of halo nuclei

J.A. Tostevin, J.S. Al-Khalili, J.M. Brooke, and J.A. Christley[1]

[1]*Department of Physics, School of Physical Sciences, University of Surrey, Guildford, Surrey, GU2 5XH, United Kingdom*

(Dated: November 5, 2011)

Abstract

Theories of reactions of composite nuclei simplify considerably at energies of several 100 MeV/nucleon. Here Glauber methods provide a quantitative microscopic framework with a clear delineation of nucleon-nucleon scattering and nuclear structure inputs. However further approximations, tested for stable nuclei, are inappropriate for few-body halo nuclei with implications for analyses of both total reaction and elastic scattering cross sections. At lower projectile energies, of order tens of MeV/nucleon, reactions are more usefully formulated in terms of the optical interactions of the projectile constituents and the target, however corrections to Glauber theory are now large. A framework for improving such calculations at lower energies is also presented.

PACS numbers: PACS numbers: 24.10.-i, 24.10.Eq, 24.50.+g, 25.10.+s

I. FEW-BODY CALCULATIONS AT HIGH ENERGY

Neutron dripline nuclei have very weak binding of the last neutron(s). There is therefore a very large amplitude for finding these valence nucleons in the classically-forbidden region beyond a tightly bound core – producing well developed few-body structures. The root mean squared (rms) matter radii of such nuclei are therefore large, manifest empirically as large interaction/reaction cross sections with a target probe. Such data remain the clearest experimental signature of these novel structures [1], however new data, on elastic scattering of neutron-rich light nuclei from both proton and more massive targets, also demonstrate significant sensitivity to the halo size, e.g. [2, 3].

Good examples are the experimental data of the IKAR collaboration [4] on p+^{6}He and ^{8}He scattering near 700 MeV, shown in Figure 1 as a function of the momentum transfer squared, $q^2 = -t$. The data have been scaled, as indicated, to coincide at small q^2 and with the available $p + \alpha$ data. The lines are to guide the eye. Qualitatively, the increasing size of the He isotopes with A is clear, but data for a stable nucleus of known size, such as ^{6}Li, would help provide a scale for comparison with the neutron-rich systems. The rms size of ^{6}He deduced from these data in ref. [4] (2.30±0.07 fm) is less than one would expect. It suggests ^{6}He is actually smaller than ^{6}Li (with deduced matter radius of 2.44 fm from electron scattering [5]), whereas interaction cross section measurements at 800 MeV/nucleon yield a cross section for ^{6}He+^{12}C [6] (722 ± 5 mb) significantly greater than for ^{6}Li+^{12}C [7] (688 ± 10 mb).

It was already shown, in total reaction cross section calculations [8–10], that an explicit treatment of the few-body degrees of freedom of such light nuclei is of considerable quantitative importance. These few-body effects were shown to increase the transparency of the elastic S-matrix $\mathcal{S}_A(b)$ at large impact parameters b [9] leading to smaller calculated reaction cross sections – and hence to larger deduced nuclear sizes from comparisons with data. Whereas a matter radius for ^{6}He consistent with a simplified (one-body density based) analysis was 2.33 fm [1], the value 2.54 fm is consistent with a more careful few-body analysis [10] of the same experimental datum.

Since, in a projectile-target (of mass A) collision, the reaction cross section

$$\sigma_R(A) = 2\pi \int_0^\infty db\, b \left[1 - |\mathcal{S}_A(b)|^2\right] \ , \tag{1}$$

and the elastic scattering amplitude, at momentum transfer q,

$$f_A(q) = ik \int_0^\infty db\, bJ_0(qb)\ [1 - \mathcal{S}_A(b)]\ , \tag{2}$$

are both integrals involving $\mathcal{S}_A(b)$ and different weight functions, analogous few-body corrections are anticipated in elastic scattering. Here k is the projectile's incident wave number in the centre of mass (c.m.) frame. We discuss briefly a first treatment of these few-body degrees of freedom in calculations of p+^{A}He scattering at energies near 700 MeV, and their implications for the sizes of the He isotopes deduced from the experimental data [4].

A. Few-body methodology

According to Glauber's multiple scattering theory [11], the elastic amplitude for $p + A$ scattering is given by Eq. (2) where the elastic S-matrix at c.m. impact parameter b, is

$$\mathcal{S}_A(b) = \langle \Phi_A | \prod_{j=1}^{A} S_j(b_j) | \Phi_A \rangle\ . \tag{3}$$

Here j labels the target nucleons with ground state many-body wavefunction Φ_A, but, as the proton scattering experiments of ref. [4] were performed in inverse kinematics, $|\Phi_A\rangle$ is the projectile ground state. The $S_j(b_j) = 1 - \Gamma_{pj}(b_j)$ are the pairwise nucleon-nucleon scattering operators, b_j is the impact parameter of the incident proton relative to target nucleon j. Index j also identifies the use of the pn or pp profile function, Γ_{pj}. These are parameterised, as is usual, directly from the free pp and pn scattering data. For details see [3, 12].

It must be realised that $\mathcal{S}_A(b)$ is a many-body matrix element of the projectile's many-body density $|\Phi_A|^2$. It has been common practice however, e.g. [4], based on successful analyses for stable (tightly bound) nuclei [13, 14], to replace these many-body densities by products of one-body densities – sometimes putting back c.m. correlations by hand in an approximate way [14]. While for the compact ^{4}He system this is not unreasonable, and is used here, the particular spatial correlations of the nucleons in ^{6}He and ^{8}He, into a $T = 0$ α core and a neutron halo/skin component, makes such an (uncorrelated) factorisation an uncertain and unquantified procedure.

For halo nuclei, with their well developed few-body structures, an alternative n-cluster description is appropriate. Due to the weak valence nucleon binding, the expectation is also that core polarisation effects are small, particularly for the He isotopes [15]. The many-body

wavefunction is then a product of an intrinsic wavefunction Φ_{A_c} for the mass A_c core and an n-body wavefunction $\psi^{(n)}_{\rm rel}$ describing the relative motion of all clusters. The n-cluster variant of the A-body S-matrix element is thus

$$\mathcal{S}^{(n)}_A(b) = \langle\, \psi^{(n)}_{\rm rel} \,|\, \mathcal{S}_{A_c}(b_c) \prod_{j=1}^{n-1} S_j(b_j) \,|\, \psi^{(n)}_{\rm rel} \,\rangle \ , \tag{4}$$

where $\mathcal{S}_{A_c}$ is the free p+core elastic S-matrix at the same incident energy per nucleon, given by Eq. (3) with $A = A_c$.

B. Results for p+^{A}He scattering

Within this few-body model the scattering of the n-cluster nucleus is seen to be *predicted*, without free parameters, given (i) the scattering of the constituents, and (ii) their relative motion wave function $\psi^{(n)}_{\rm rel}$. Critically however $\mathcal{S}^{(n)}_A$ remains a many-body matrix element, now of the projectile's few-body density $|\psi^{(n)}_{\rm rel}|^2$, and, in general, has no simple relationship to the projectile's one-body density.

The calculated $p + \alpha$ S-matrix, $\mathcal{S}_4$, using a simple (c.m. correlated) $(0s)^4$ oscillator four-body α density

$$|\Phi_4(\vec{r}_1, \vec{r}_2, \vec{r}_3, \vec{r}_4)|^2 \propto \prod_{j=1}^{4} |\phi(r_j)|^2 \, \delta(\vec{r}_1 + \vec{r}_2 + \vec{r}_3 + \vec{r}_4) \tag{5}$$

reproduces the 699 MeV $p + \alpha$ data of Figure 1 [3] for an α rms matter radius of 1.49 fm, consistent with electron scattering [5], and is not shown. To calculate $\mathcal{S}_4$ the S_j used is the $(T = 0)$ average of the pn and pp amplitudes. Given $\mathcal{S}_4$ and Γ_{pn} all inputs to the ^{6}He and ^{8}He calculations, other than the relative motion wavefunctions $\psi^{(n)}_{\rm rel}$, are completely determined.

Figure 2 shows the *predicted* p+^{6}He elastic cross sections at 717 MeV using three (P1, FC and GB3) Faddeev wavefunction models $\psi^{(3)}_{\rm rel}$ tabulated in [9]. These yield ^{6}He radii of 2.33, 2.50, and 2.77 fm, respectively, assuming an α rms radius of 1.49 fm. The figure shows that the elastic scattering data are consistent with the FC-model wavefunction with rms radius 2.50 fm. The data are subject to a normalisation uncertainty of order $\pm 3\%$ [4]. The inset shows the calculated total reaction cross sections as a function of the ^{6}He rms matter radius for several wavefunction models. These show significant sensitivity and, if accessible experimentally, could provide a powerful constraint in combination with the q^2 data.

The approximate (one-body density) analysis of [4] and the few-body analysis above lead to quite different outcomes. While the density-based calculations suggest a radius of 2.30 fm is appropriate [4], the more careful few-body treatment of the reaction suggests a radius of order 2.50 fm. We comment that the FC wavefunction also reproduces the experimental ^{6}He+^{12}C interaction cross section datum at 800 MeV/nucleon in the careful finite range study of that process [10]. The FC model also reproduces most closely the empirical ^{6}He three-body binding energy of 0.97 MeV.

Five-body ($\alpha + 4n$) descriptions of ^{8}He are less readily available. Here we assume for $\psi^{(5)}_{\rm rel}$ the COSMA wavefunction of [16], however the original $(0p)^4$ oscillator valence neutron wavefunctions are now matched smoothly to a p-wave Hankel function tail. As the two-neutron separation energy from ^{8}He is 2.137 MeV and the four-neutron separation energy is 3.1 MeV, we assume an average separation energy of 1 MeV for this purpose. The wavefunction is then renormalised to unity and the ^{8}He matter radius of is computed.

Our first calculations for this system are collected in Figure 3 which shows the *predicted* p+^{8}He elastic cross section at 674 MeV. The calculations correspond to the ^{8}He rms matter radii indicated. Calculations for radii in the range 2.4–2.5 fm, suggested by the analysis of [4], do not reproduce the experimental data. A radius of 2.6 fm is consistent with the data within the COSMA model used. Again the inset shows the calculated total reaction cross sections as a function of the ^{8}He rms matter radius. As for ^{6}He these reveal a significant sensitivity to the projectile size.

We observe significant sensitivity in the calculated cross section to the wavefunction asymptotics and conclude, quite generally, that a careful and realistic treatment of these few-body systems will be essential to making quantitative deductions from comparisons with such data.

II. FEW-BODY CALCULATIONS AT LOW ENERGY

We now consider calculations for few-body projectiles at energies of a few 10's of MeV per nucleon. At these lower energies the reaction mechanisms are more complex and the interactions in the two-body subsystems are best deduced, as far as possible, from empirical data and established theoretical models for stable nuclei. Recent calculations for ^{8}He+^{12}C scattering [17], as well as those above for p+^{8}He scattering – treated as six-body problems

– show that the Glauber models provide an effective basis for the calculation of reactions of few- and many-body projectiles. This efficiency arises from the very simple (independent scattering) nature of each two-body input. This efficiency warrants an investigation of corrections to the model in an attempt to extend its accuracy.

^{11}Be and ^{6}He are good examples of single-neutron and two-neutron halo nuclei. Some elastic scattering data are also available for both systems in the energy region of interest. For two-body projectiles [18], and very recently for three-body projectiles [19], full quantum mechanical calculations, which use the adiabatic approximation but not the Glauber/eikonal and independent scattering assumptions, are possible. These will be used to assess the nature of corrections to the lowest order theory.

For an n-body projectile scattering from a target nucleus, rather than a proton, the elastic amplitude is given, as previously, by Eqs. (2) and (3) but where now the S_j are the Glauber S-matrices for each constituent j-target subsystem, interacting via a potential V_j. Explicitly [11]

$$S_j(b) = \exp[i\chi_j^0(b)] \quad , \qquad \chi_j^0(b) = -\frac{1}{\hbar v}\int_{-\infty}^{\infty} V_j(\sqrt{b^2+z^2})dz \quad , \tag{6}$$

where v is the asymptotic relative velocity and the z-axis is in the incident beam direction. χ_j^0 is referred to as the eikonal phase.

A. Beyond the eikonal model

Following Wallace [20] and others, we have recently made use of the correspondence between the eikonal phase and the WKB phase shift χ_j^W. The latter can be expanded, in powers of $\epsilon = 1/\hbar kv$, about the eikonal phase [21]

$$\chi_j^W(b) = \sum_{n=0}^{\infty} \frac{\epsilon^n}{(n+1)!}\chi_j^n(b), \quad \chi_j^n(b) = -\frac{1}{\hbar v}\int_{-\infty}^{\infty} dz \left(\frac{1}{r}\frac{d}{dr}\right)^n [r^{2n}V_j(r)^{n+1}] \ , \tag{7}$$

which is the $n = 0$ term. The χ_j^W require correction terms χ_j^{RY}, as clarified by Rosen and Yennie [22].

We have shown [23] that improving the phase in each S_j of the few-body model, by replacing the eikonal phase χ_j^0 by $\chi_j^W + \chi_j^{RY}$, leads to significant changes and improvements in calculations, when compared with exact adiabatic results. Doing this retains the *independent scattering* nature of the lowest order theory and so neglects "overlapping potential" terms

[24]. The indications from our calculations [23] are that such terms, from configurations in which both core and valence particles overlap the target, are very small for extended halo nuclei with a strongly absorbed core particle.

Having established that the non-eikonal corrections are large, one finds that the expansions involved in calculating the constituent $\chi_j^W + \chi_j^{RY}$ converge only very slowly to the exact (partial wave) phases as the projectile energy is reduced. Figure 4 shows $|S_n(b)|$, for n+^{12}C at 25 MeV, calculated in the eikonal model (dot-dashed), the WKB and RY corrected model (dashed), up to $n = 3$ terms, and the exact partial wave values (points and solid line) where $kb = \ell + \frac{1}{2}$. Rather than sum this expansion we therefore propose to solve the radial Schrödinger equation, for each constituent j, at the required impact parameters b, and hence non-integer angular momenta $\lambda = bk_j - \frac{1}{2}$. The $S_j(b)$ are then obtained by matching, in the normal manner, to the asymptotic solutions, analytically continued for real non-integer λ, i.e.

$$\psi_\lambda^j(R) \rightarrow \frac{i}{2}\left[H_\lambda^{(-)}(k_jR) - S_j(b)H_\lambda^{(+)}(k_jR)\right] \ . \tag{8}$$

We refer to this procedure as an impact parameter multiple scattering (IPMS) approximation. The differences between few-body calculations using these independent S_j and exact (non-eikonal) adiabatic calculations provide a measure the importance of the neglected terms due to overlapping potentials, or correlated scattering.

B. Comparisons of eikonal and non-eikonal calculations

Figure 5 shows calculated elastic differential cross sections (ratio to Rutherford) for ^{11}Be+^{12}C scattering at 50, 25 and 10 MeV/nucleon for selected two-body interactions V_j [23]. The dot-dashed curves show the results of the lowest order eikonal model calculation. The IPMS results are shown by the long-dashed curves which are seen to agree to high precision, at even the lowest energy, with the exact three-body adiabatic model calculations [18], shown by the solid curves. Figure 6 shows analogous elastic differential cross section (ratio to Rutherford) calculations for ^{6}He+^{12}C scattering at 41.6 and 25 MeV/nucleon. Again the dot-dashed curves are the results of the lowest order eikonal model calculations. The IPMS results are shown by the long-dashed curves and the exact four-body adiabatic model calculations [19] by the solid curves. The IPMS calculations are performed in a small fraction of the time of the coupled channels adiabatic solutions and are readily generalised to

many-body systems.

We conclude that the IPMS framework provides an effective procedure to enhance the accuracy of few-body Glauber model calculations at low energies for one and two-neutron halo nuclei. It remains to be tested, for a neutron skin nucleus such as ^{8}He with several valence neutrons in a more confined volume, whether this independent scattering picture remains as accurate.

III. SUMMARY

We have discussed briefly the need for quantitative calculations of few-body scattering and reactions at energies from 10's MeV to 1 GeV/nucleon, to confront experimental data of increased novelty and precision. We have shown that, within a few-body model of ^{6}He, the recent p+^{6}He elastic scattering data at 700 MeV are consistent with the same three-body ^{6}He wavefunction that reproduces the interaction cross section measurement for ^{6}He+^{12}C at 800 MeV/nucleon. The deduced ^{6}He and ^{8}He sizes from the few-body calculations are 0.2 fm larger than those reported from the more approximate analysis of ref. [4].

We have also shown that, in the adiabatic approximation, even at very low energies, to high accuracy halo nuclei behave as if the constituent particles scatter independently, suggesting a simple practical framework for increasing their accuracy. This is shown to work well for one- and two-neutron halo nuclei.

Acknowledgments

The financial support of the United Kingdom Engineering and Physical Sciences Research Council (EPSRC) in the form of Grant No. GR/J95867, of a research studentship (for JMB), and of a Royal Society Travel Grant are gratefully acknowledged.

---

[1] I. Tanihata *et al.*, Phys. Lett. **B160** (1985) 380; **B206** (1988) 592.

[2] R.C. Johnson, J.S. Al-Khalili and J.A. Tostevin, Phys. Rev. Lett. **79** (1997) 2771.

[3] J.S. Al-Khalili, J.A. Tostevin, *Few-body calculations of p-^{6,8}He scattering*, submitted 11/97.

[4] G.D. Alkhazov *et al.*, Phys. Rev. Lett. **78**, (1997) 2313.

[5] H. de Vries, C.W. de Jager and C. de Vries, At. Data Nucl. Data Tables **36** (1987) 495.

[6] I. Tanihata, D. Hirata, T. Kobayashi, S. Shimoura, K. Sugimoto and H. Toki, Phys. Lett. **B289** (1992) 261.

[7] I. Tanihata *et al.*, Phys. Rev. Lett. **55** (1985) 267.

[8] J.S. Al-Khalili and J.A. Tostevin, Phys. Rev. Lett. **76** (1996) 3903.

[9] J.S. Al-Khalili, J.A. Tostevin and I.J. Thompson, Phys. Rev.C **54** (1996) 1843.

[10] J.A. Tostevin and J.S. Al-Khalili, Nucl. Phys. **A616** (1997) 418c.

[11] R.J. Glauber, *Lectures in Theoretical Physics*, (Interscience, N.Y., 1959) Vol. 1, 315.

[12] L. Ray, Phys. Rev. C **20** (1979) 1857.

[13] S. Kox *et al.*, Phys. Rev. C **35** (1987) 1678.

[14] G.D. Alkhazov, S.L. Belostotsky and A.A. Vorobyov, Phys. Rep. **42C** (1978) 89.

[15] T.T.S. Kuo, F. Krmpotić, and Y. Tzeng, Phys. Rev. Lett. **78** (1997) 2708.

[16] M.V. Zhukov, A.A. Korsheninnikov and M.H. Smedberg, Phys. Rev. C **50** (1994) R1.

[17] J.A. Tostevin, J.S. Al-Khalili, M. Zahar, M. Belbot, J.J. Kolata, K. Lamkin, D.J. Morrissey, B.M. Sherrill, M. Lewitowicz, and A.H. Wuosmaa, Phys. Rev. C **56** (1997) 2929R.

[18] H. Amakawa, S. Yamaji, A. Mori and K. Yazaki, Phys. Lett. **82B** (1979) 13.

[19] J.A. Christley, J.S. Al-Khalili, J.A. Tostevin, R.C. Johnson, Nucl. Phys. **A624** (1997) 275.

[20] S.J. Wallace, Phys. Rev. D **8** (1973) 1846.

[21] S.J. Wallace, Ann. Phys. (N.Y.) **78** (1973) 190; Phys. Rev. Lett. **27** (1971) 622.

[22] M. Rosen and D.R. Yennie, J. Math. Phys. **5** (1964) 1505.

[23] J.S. Al-Khalili, J.A. Tostevin and J.M. Brooke, Phys. Rev. C **55** (1997) R1018.

[24] H. Feshbach, *Theoretical Nuclear Physics: Nuclear Reactions*, (Wiley, N.Y., 1992), 103; and references therein.

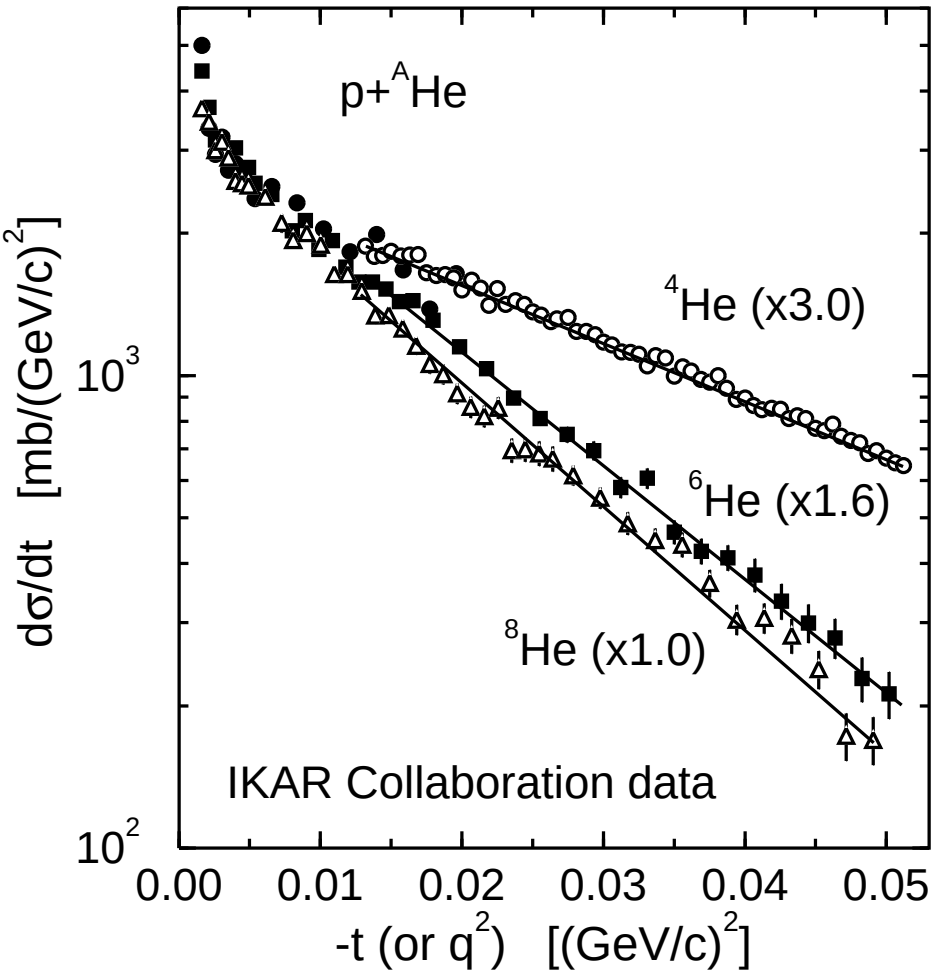

FIG. 1: FIG.1. p+^{4}He, ^{6}He, and ^{8}He data at 699, 717, and 674 MeV, respectively.

Figures

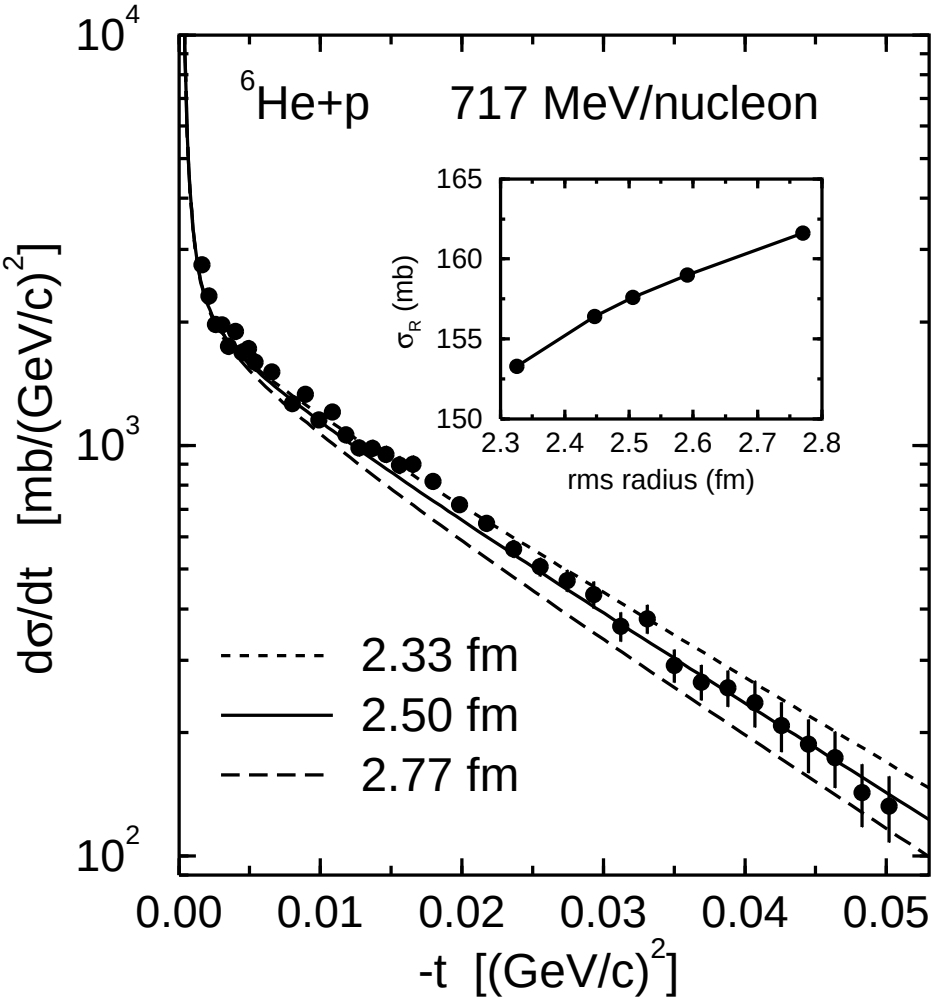

FIG. 2: FIG.2. p+^{6}He elastic differential cross sections at 717 MeV.

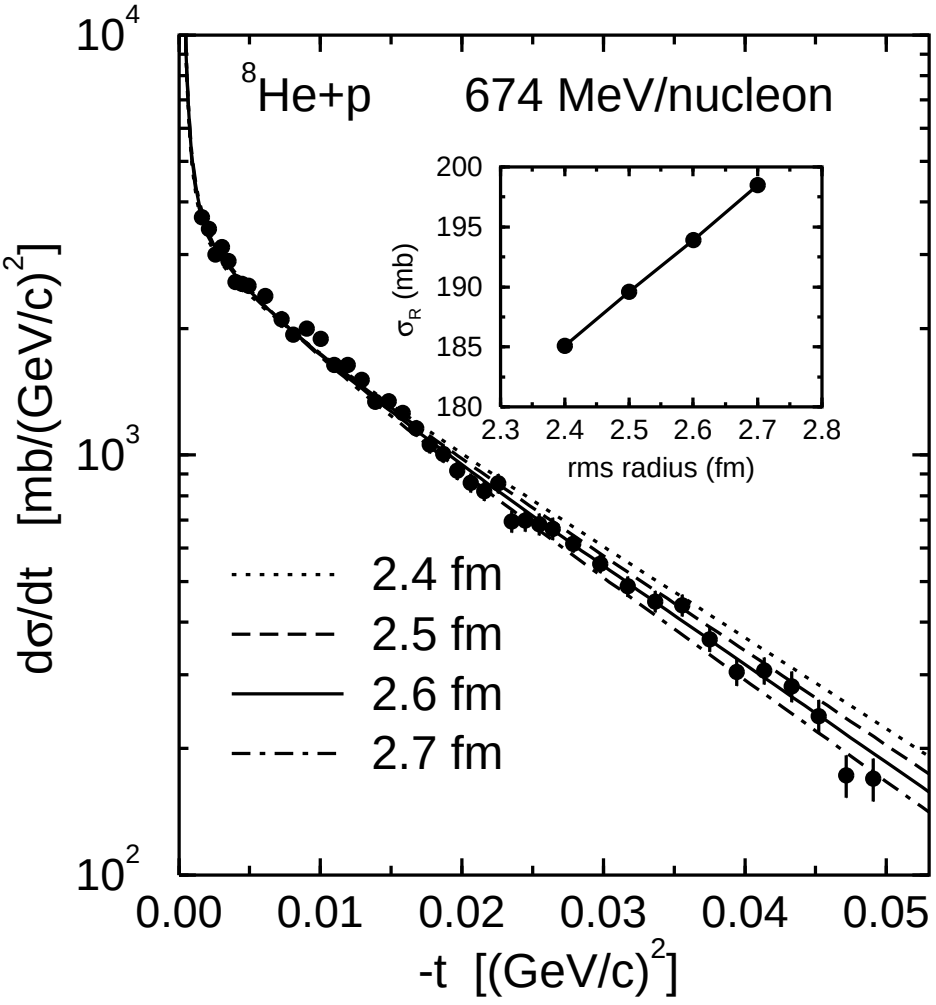

FIG. 3: FIG.3. p+^{8}He elastic differential cross sections at 674 MeV.

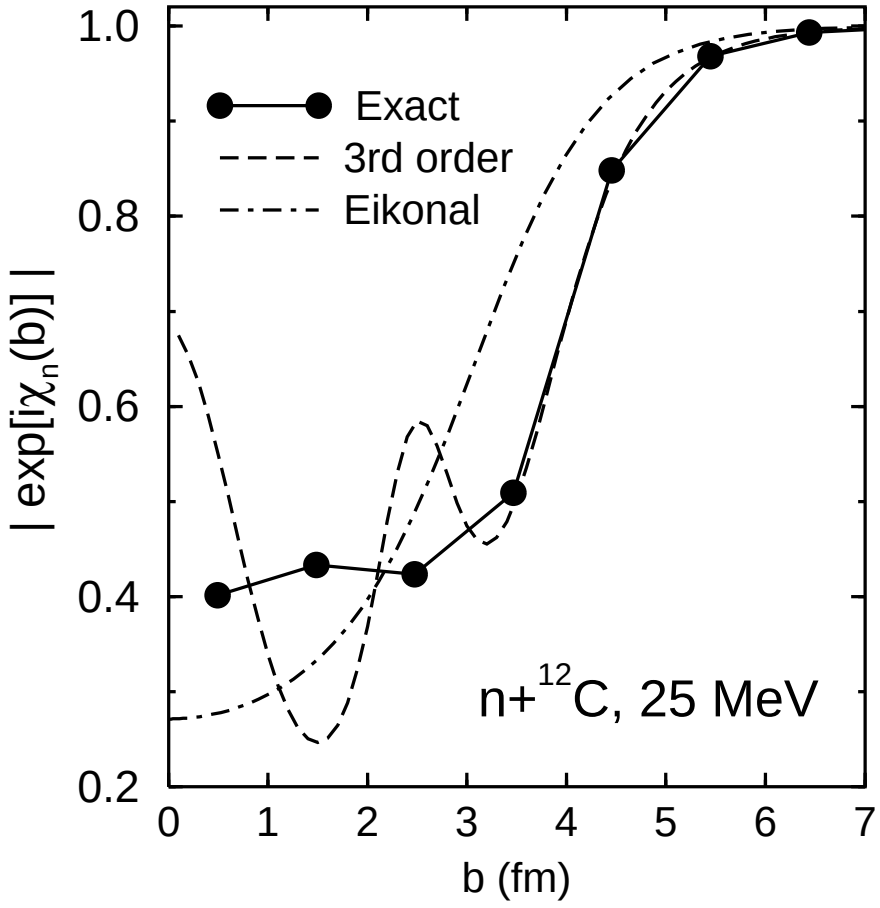

FIG. 4: FIG.4. Modulus of the n+^{12}C S-matrix at 25 MeV.

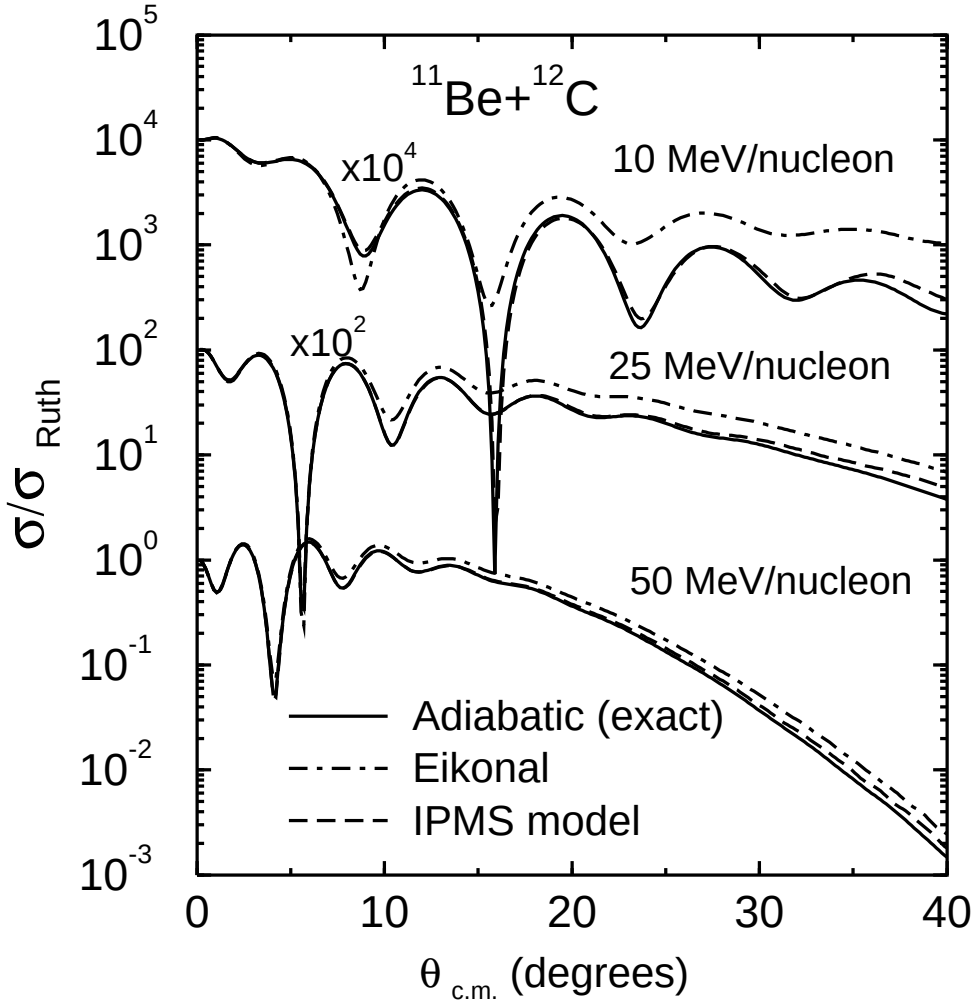

FIG. 5: FIG.5. Elastic cross sections for ^{11}Be+^{12}C.

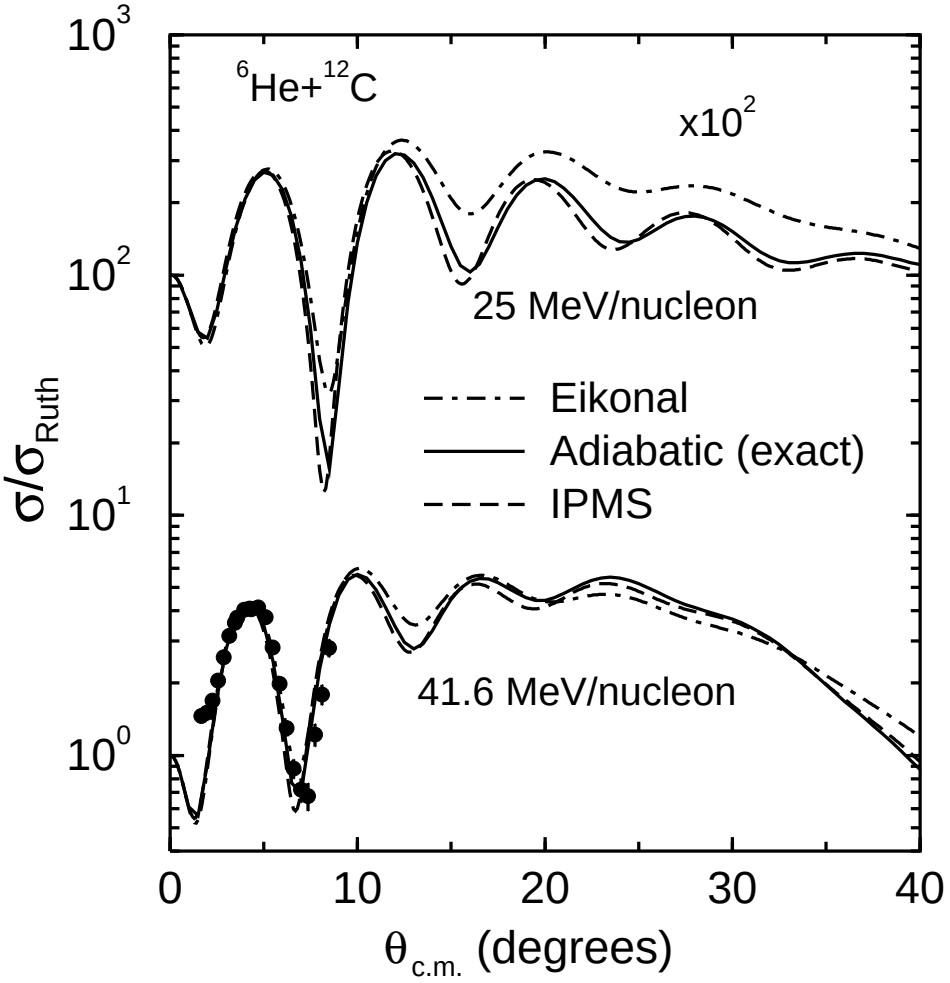

FIG. 6: FIG.6. Elastic cross sections for ^{6}He+^{12}C.